

Proton magnetic resonance spectroscopy in childhood brainstem lesions

L. Porto · E. Hattingen · U. Pilatus · M. Kieslich ·
B. Yan · D. Schwabe · F. E. Zanella · H. Lanfermann

Received: 8 February 2006 / Revised: 10 May 2006 / Published online: 16 September 2006
© Springer-Verlag 2006

Abstract

Background Diagnosis of brainstem lesions in children based on magnetic resonance imaging alone is a challenging problem. Magnetic resonance spectroscopy (MRS) is a noninvasive technique for spatial characterization of biochemical markers in tissues and gives information regarding cell membrane proliferation, neuronal damage, and energy metabolism.

Methods We measured the concentrations of biochemical markers in five children with brainstem lesions and evaluated their potential diagnostic significance. Images and spectra were acquired on a 1.5-T imager. The concentrations of *N*-acetylaspartate, tetramethylamines (e.g., choline), creatine, phosphocreatine, lactate, and lipids were measured within lesions located at the brainstem using Point-resolved spectroscopy sequences.

Results Diagnosis based on localized proton spectroscopy included brainstem glioma, brainstem encephalitis, demyelination, dysmyelination secondary to neurofibromatosis type 1 (NF 1), and possible infection or radiation necrosis. In all but one patient, diagnosis was confirmed by biopsy or by clinical follow-up.

Conclusions This small sample of patients suggests that MRS is important in the differential diagnosis between proliferative and nonproliferative lesions in patients without neurofibromatosis. Unfortunately, in cases of NF 1, MRS can have a rather misdiagnosis role.

Keywords Brainstem lesions · 1H MR spectroscopy · Magnetic resonance imaging · Children · Brainstem glioma · Brainstem encephalitis · Neurofibromatosis type 1

L. Porto · E. Hattingen · U. Pilatus · B. Yan · F. E. Zanella ·
H. Lanfermann
Neuroradiology Department,
Klinikum der Johann Wolfgang Goethe-Universität,
Frankfurt am Main, Germany

M. Kieslich
Neuropediatric Department,
Klinikum der Johann Wolfgang Goethe-Universität,
Frankfurt am Main, Germany

D. Schwabe
Pediatric Hematology/Oncology Department,
Klinikum der Johann Wolfgang Goethe-Universität,
Frankfurt am Main, Germany

L. Porto (✉)
Institut für Neuroradiologie,
Klinikum der Johann Wolfgang Goethe-Universität,
Schleusenweg 2-16,
60528 Frankfurt am Main, Germany
e-mail: luciana.porto@kgu.de

Introduction

The major diagnostic possibilities of brainstem lesions in children are brainstem glioma, encephalitis (viral, autoimmune, or protozoan), demyelination, dysmyelination secondary to neurofibromatosis type 1 (NF1), Langerhans' cell histiocytosis, hamartomas, resolving hematoma, vascular malformations, and tuberculoma [1]. The advent of magnetic resonance imaging (MRI) has simplified the diagnosis of brainstem lesions in that it allows differentiation of brainstem astrocytomas from vascular malformations and subacute hemorrhage. However, it is not possible to definitively differentiate encephalitis or a tuberculoma from brainstem tumor on MRI. Magnetic resonance spectroscopy (MRS) offers additional information on the biochemical makeup of brainstem lesions and holds promise in improving the diagnostic accuracy of MRI.

We performed MRS in all the children in this series with brainstem lesions and endeavored to establish whether MR spectroscopy is helpful in differentiating major brainstem pathologies, particularly encephalitis or demyelinating lesions from brainstem tumor.

Materials and methods

The MR images and clinical records of five children with brainstem lesions were reviewed. MR imaging and MRS were performed.

MRS was performed on a 1.5-T whole-body MR-scanner (Magnetom Vision, Siemens, Germany) using a standard circular polarized head coil. For contrast-enhancing masses, postcontrast T1-weighted images were obtained (Gadolinium-DPTA, TR=237 ms, TE=4.8 ms, pulse angle=80°). For noncontrast-enhancing tumors, T2-weighted images were obtained (TR=7,400, TE=114 ms, pulse angle=160°). Single-voxel MRS was performed using the Point-resolved spectroscopy (PRESS) volume selection with an echo time (TE) of 135 ms and a repetition time (TR) of 1,500 ms. Suppression of water signal was achieved by frequency-selective chemical shift-selective (CHESS) pulses. Sizes of volumes of interest (VOI) ranged from 2.2 to 12.7 ml and were positioned within the lesion core. The volume was adapted to the size of the lesion. The minimum extension of each side was at least 1 cm in the different directions. The reference spectrum was obtained using identical acquisition parameters from the cerebellum of normal appearance. Depending on the size of the selected VOIs, 128–256 acquisitions were added, with total acquisition times ranging from 3.25 to 6.50 min per spectrum. Before acquisition, global and localized shimming was conducted on the nonsuppressed water signal, followed by adjustment of the frequency-selective pulses for optional water suppression. The total time required for the MR-spectroscopic examination ranged from 30 to 40 min. Initially, data were analyzed on the spectrometer console using the postprocessing tools provided by the manufacturer. For quantitative analysis, data were processed off-line on a LINUX workstation using the jMRUI software (Version 2.1). The residual water signal was removed from the measured free induction decay (FID) by means of time-domain Hankel Lanczos singular value decomposition (HLSVD) filtering [18] as implemented in the MRUI package [14, 18–20].

The resulting pure metabolite FIDs were then analyzed with AMARES, a nonlinear least square fitting algorithm operating in the time domain [21]. The time-domain model function was composed of four exponentially decaying sinusoids with identical damping, corresponding to peaks in the frequency domain assigned to trimethylamines at

3.24 ppm (mainly choline, phosphocholine, and glycerophosphocholine, abbreviated as Cho), creatine at 3.05 ppm (Cr, originating from creatine and phosphocreatine), *N*-acetylaspartate (NAA), and *N*-acetylaspartate-glutamate (NAAG) at 2.03 and 2.05 ppm, plus seven exponentially damped sinusoids that accounted for all other resonances present in the spectrum (e.g., lactate or lipid at 1.3 ppm), to optimize the fitting of the resonances of interest. Since no clear distinction between NAA and NAAG can be achieved, both metabolite intensities were added up to tNAA. Intensities of Cho, tCr, and NAA were quantified as ratios between the lesion and the cerebellum. In addition, the ratio between NAA and total creatine (NAA/tCr) and the ratio between choline and total creatine (CHO/tCr) within the lesion were calculated and used for interpretation of the data.

Spectroscopic inclusion criteria were the following: (1) A maximum partial volume effect of 10% was accepted (a maximum of 10% of nonmass area within the VOI, determined volumetrically). (2) Local field inhomogeneities were accepted with a line broadening of less than 10 Hz full-width at half maximum. (3) No artifacts due to movement of the patient. (4) A sufficient reference spectrum was obtained using identical acquisition parameters from the cerebellum of normal appearance. (5) There had to be sufficient water suppression and no extravoxel lipide contamination to avoid inaccurate quantification of the resonances for choline, lipide, lactate, and NAA.

There was no overlap between the control spectra and the brainstem abnormality spectra.

Results

Data on clinical information and lesion location as well as data on imaging findings and outcome are presented in Tables 1 and 2 (see Figs. 1, 2, 3, 4 and 5).

Discussion

Childhood brainstem lesions are difficult to evaluate with MRI. Importantly, this is an area of the brain where biopsy is dangerous. In contrast to MRI and CT, MRS provides completely different information regarding neural integrity, cell proliferation, cell degradation, energy metabolism, and necrotic transformation of brain or tumor [12, 13].

It is generally recognized that NAA is a marker of functional neurons and their appendages. When brain tissue is damaged or replaced by any destructive, degenerative, or infiltrative process, NAA is markedly reduced [5, 10, 11, 23]. Since Cr-bound phosphates are a substrate of the ATP/ADP cycle, Cr is considered an indicator of energy

metabolism. In addition, Cr is believed to be relatively constant in various metabolic conditions, it has often been used in previous studies as an internal standard for semiquantitative evaluation of metabolic changes of other brain metabolites. However, the use of a ratio will result in loss of metabolic information since a ratio does not change when both the numerator and the denominator alter equally, nor does a ratio reveal the direction of the changes. Furthermore, working with only a metabolite ratio will not take into account the known regional and age-dependent differences in metabolite signals. Therefore, we have calculated the ratios from the same metabolite (e.g., NAA) measured in the lesion core and the normal appearing cerebellum as an internal standard.

Cho resonances originate mainly from intermediates of phospholipid metabolism such as phosphocholine and glycerophosphocholine. Both metabolites play an important role in the structure and function of cell membranes. Consequently, increased Cho can be seen in processes with elevated cell-membrane turnover, such as in proliferating tumors and in the developing brain. Lipids and lactate are physiologically not detectable in healthy brain. Studies have shown that the amount of lipids detected by spectroscopy correlates well with the degree of micro- and macro-necrosis seen on histology [24]. Brain lactate is produced in conditions of anaerobic glycolysis. It is a result of a mismatch between glycolysis and oxygen supply and

indicates hypoxic conditions and hypermetabolic glucose consumption.

Although as many as 43% of patients with NF 1 will show hamartomas by MR imaging, fewer than 10% of the lesions show growth on serial examinations [4]. Of note, there appears to be no correlation between the number and location of these lesions with the clinical status of the patients. Therefore, it is important to differentiate hamartomas from low-grade astrocytomas. Obviously, early detection of astrocytomas is desirable. Jones et al. [8] reported that focal brain lesions in patients with NF 1 could be separated into two groups, one demonstrating only slight metabolite ratio changes relative to normal brain and the other group showing significant increase in choline and decrease in NAA. In this latter group of patients, regression of a previously identified lesion was noted. The significant increase in Cho/Cr ratios and in the Cho levels, as in our patient 1, is unexpected, as an increase in Cho is often seen in the presence of rapidly dividing cells and Cho is increased in all primary and secondary brain tumors. It is therefore perhaps surprising to encounter this change in what are considered to be benign, asymptomatic lesions. Wang et al. [22] postulated that Cho elevations reflect increased myelin turnover in areas of intramyelinic edema, which is followed by neuropil injury (reduced NAA). This assumption is in agreement with their report of elevated Cho and relatively preserved NAA within unidentified

Table 1 Clinical information and lesion location

No.	Age/ gender	Diagnosis	Symptoms	No. of lesions	Location
1	4 years old/F	NF 1	Positive family history and visual failure	2	1. Brainstem mass with extension to the right cerebellar peduncle 2. Optic chiasm/hypothalamus astrocytoma
2	8 years old/M	BS glioma, confirmed by open biopsy	Fever, vomiting, dysphagia, slurred speech, and disequilibrium	1	Brainstem mass with extension to the cerebellum
3	5 years old/M	Presumed BS encephalitis. CSF was unremarkable. Oligoclonal bands and mitochondrial tests were negative.	Left-sided horizontal and vertical nystagmus, double vision, and disequilibrium after coryzal illness	1	Hyperintensity in the tegmentum of the pons and mesencephalon
4	11 years old/F	Positive oligoclonal bands confirming the diagnosis of MS	Right-sided weakness and disequilibrium; bilateral cerebellar signs	Multiple	Lesions in the white matter, in the left basal ganglia, on the left side of the brainstem, and in middle cerebellar peduncle
5	15 years old/F	Presumed infection or radiation	Acute left hemiparesis and ataxia, which progressed in the next 48 h; previous history of low-grade pineocytoma and radiation therapy	2	Stable small cystic changes in the region of the glandula pinealis; new abnormality in the right upper pons

BS brain stem, MS multiple sclerosis, NF 1 neurofibromatosis type 1

Table 2 Imaging findings and outcome

No.	MR: Brainstem abnormalities	MRS findings	Outcome after treatment
1	<p>1. Hyper mass in the brain stem with extension to the right cerebellar peduncle and mass effect on the floor of the fourth ventricle</p> <p>2. MRI control after 5 months showed increased mass effect of the BS lesion.</p>	<p>1. Decreased levels of NAA and Cr while Cho was only moderately elevated (Fig. 1c). MRS findings were suggestive of “hamartoma,” but such values of metabolites could be also suggestive for low-grade astrocytoma.</p> <p>2. The follow-up MRS showed decreased levels of NAA while Cho levels showed a steep increase (approx 290% compared to the normal appearing parenchyma), suggestive of high-grade glioma (Fig. 1e).</p> <p>3. Later MRS control, after 14 months without any specific therapy, showed reduction of the Cho levels, but it remained within high levels (approx 200% compared to the normal appearing parenchyma).</p>	The patient after 18 months without aggressive treatment is doing well with no increase in the brain stem mass.
2	Abnormal signal and enhancement within the brain stem and cerebellum (Fig. 2a and b)	Decreased levels of NAA with elevated Cho and Cr, compatible with high-grade glioma (Fig. 2c)	Died
3	Isolated prolongation of T2 signal in the tegmentum of the pons and mesencephalon (Fig. 3a and b) without enhancement after contrast. MRI 1 week later showed complete regression of the prolonged T2 signal.	MRS at the time of MRI control showed a normal spectrum without increased lactate or choline (Fig. 3c).	The child was treated with corticosteroid and showed clinical improvement. After 4 years, there was no further clinical relapse.
4	Multiple hyper lesions in the white matter, in the left basal ganglia, on the left side of the brainstem, and in the middle cerebellar peduncle (Fig. 4a–c).	Decreased level of NAA (Fig. 4d). Cho was only mildly elevated. MRI and MRS suggested demyelination.	Improved with therapy
5	Round area of signal abnormality in the right upper pons, which was hyper on DWI (Fig. 5c). The lesion showed a ring-like enhancement after contrast (Fig. 5b). On the T2, 6 months later, the lesion was mildly hypo, suggesting small areas of hemorrhage with occult vascular malformation (Fig. 5d). MR with DWI findings was suggestive of pontine infarction, but neither infection nor radiation necrosis could not be ruled out.	MRS (Fig. 5d) showed decreased level of NAA and Cr. Cho was not elevated. A lipid peak and moderate elevation of lactate were seen. The diagnosis was presumed to be either infection or radiation. Importantly, a proliferative process was ruled out by reason that MRS showed an absence of choline peak.	Improved

Iso indicates on MR isointense; hypo, hypointense; and hyper, hyperintense

BS brain stem, DWI diffusion-weighted imaging, MS multiple sclerosis, MR/MRI magnetic resonance imaging, MRS magnetic resonance spectroscopy, NF 1 neurofibromatosis type 1, T1 T1-weighted images, T2 T2-weighted images

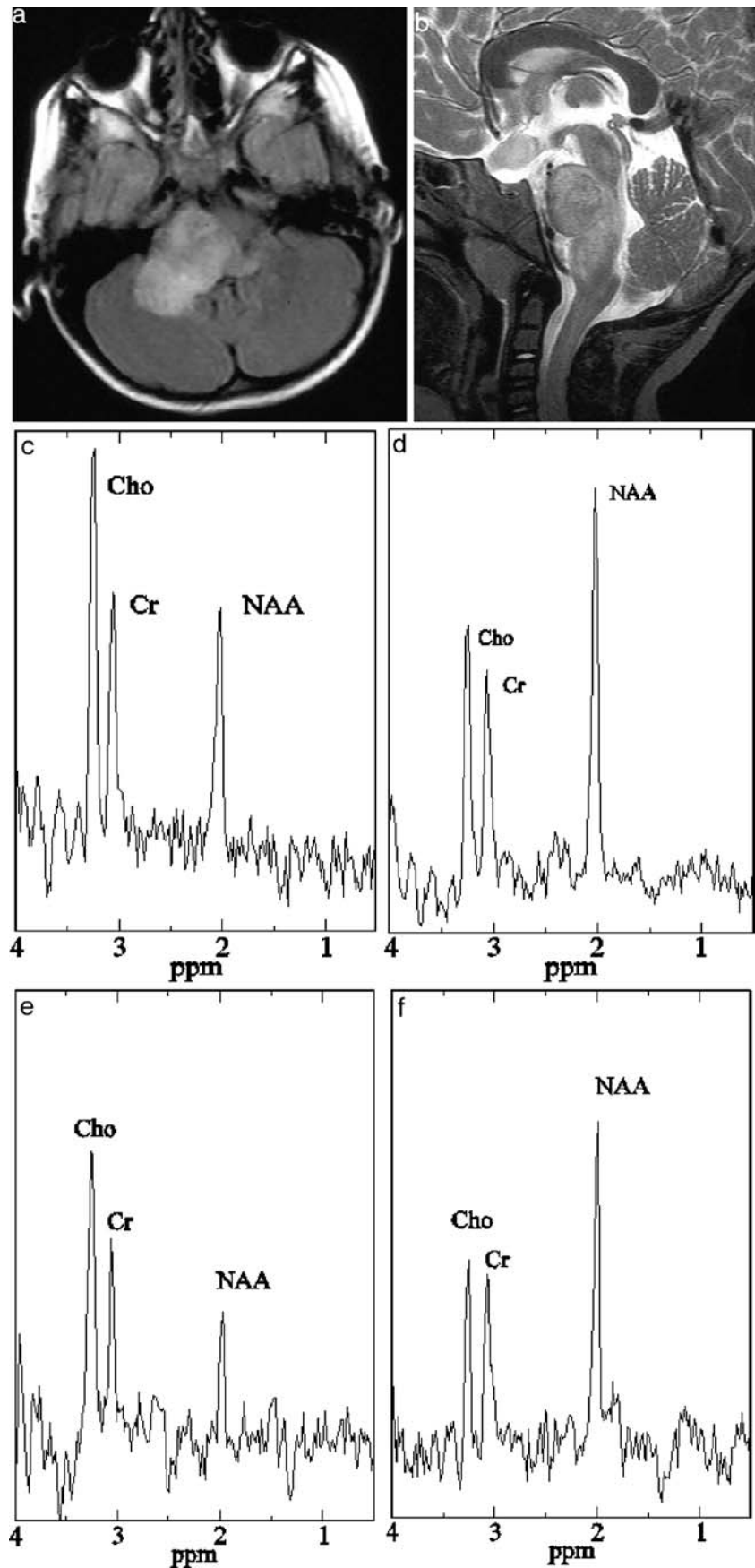
neurofibromatosis objects (UNOs) in younger patients (<10 years) and normal Cho in older subjects.

With the knowledge that high Cho levels within UNOs can be seen in younger patients with NF, an MRS control after 14 months without any aggressive therapy was done, which showed moderate but significant decrease in the Cho levels without change in the morphology or size of the brainstem mass. We presume that the brainstem lesion in patient 1 was in fact a result of an increased myelin turnover in areas of intramyelinic edema, with subsequent spontaneous reduction of the Cho levels. Brain lesions in

patients with NF 1 deserve further investigation with temporal analyses at MRS.

Several former studies [5, 10, 11, 23] observed a common feature of primary and metastatic brain tumor with increased Cho and decreased NAA. In the case of patient 2, the initial diagnosis was acute infectious or autoimmune encephalitis. MRI showed abnormal signal in the pons and cerebellar hemispheres (Fig. 2a and b). MRS (Fig. 2c) showed significantly decreased levels of NAA. Cho (249%) was markedly elevated. Due to diminished NAA level and relatively high Cr level, the NAA/Cr ratio

Fig. 1 A 4-year-old girl with visual failure. **a** Axial FLAIR image shows a hyperintense mass in the brain stem with extension to the right cerebellar peduncle and mass effect on the floor of the fourth ventricle. **b** Midsagittal T2-weighted image shows the brain stem mass and a second hyperintense mass in the region of the optic chiasm/hypothalamus compatible with optic chiasm/hypothalamus astrocytoma. **c, d** *Left spectrum*: brain stem mass lesion. *Right spectrum*: normal cerebellum. Values of NAA (2.0 ppm), Cr (3.0 ppm), and Cho (3.2 ppm) reflect signal peak integrals (arbitrary units). Metabolite levels relative to the contralateral normal cerebellum: NAA 53%; Cr 91%; Cho 117%. Levels of NAA and Cr are decreased while Cho is only moderately elevated compatible with hamartoma. **e, f** Control spectrum after 5 months. **e** *Left spectrum*: brain stem mass lesion. **f** *Right spectrum*: normal cerebellum. The left spectrum shows NAA reduction to 30% with significant increase in Cho levels (approx 290%). The NAA/Cr ratio is very low (0.3; normal, 1.73), due to diminished NAA and relatively high Cr level. These findings were suggestive of high-grade glioma, probably grade III. Further control after 14 months without therapy showed reduction of the Cho levels



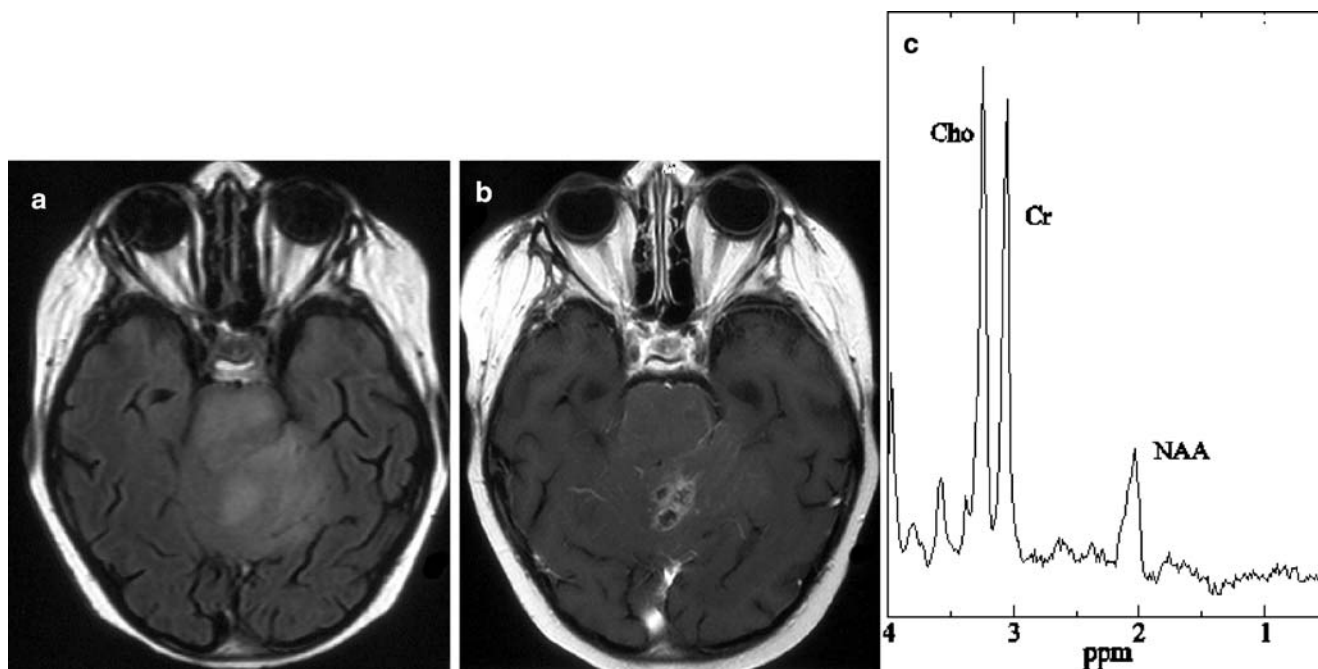


Fig. 2 An 8-year-old boy with vomiting, slurred speech, and disequilibrium. **a** Axial FLAIR image shows abnormal signal in the pons and cerebellar hemispheres, with the left side more involved than the right. **b** Axial T1-weighted contrast enhanced MR image shows regions of enhancement in the cerebellum. **c** Spectrum of brain stem mass lesion. Values of NAA (2.0 ppm), Cr (3.0 ppm), and Cho

(3.2 ppm) reflect signal peak integrals (arbitrary units). Metabolite levels relative to the contralateral normal cerebellum: NAA 31%; Cr 163%; Cho 249%. No lactate peak. Levels of NAA are decreased while Cho are significantly elevated compatible with high-grade glioma. The NAA/Cr ratio is very low (0.32; normal, 1.73) due to diminished NAA and relatively high Cr level

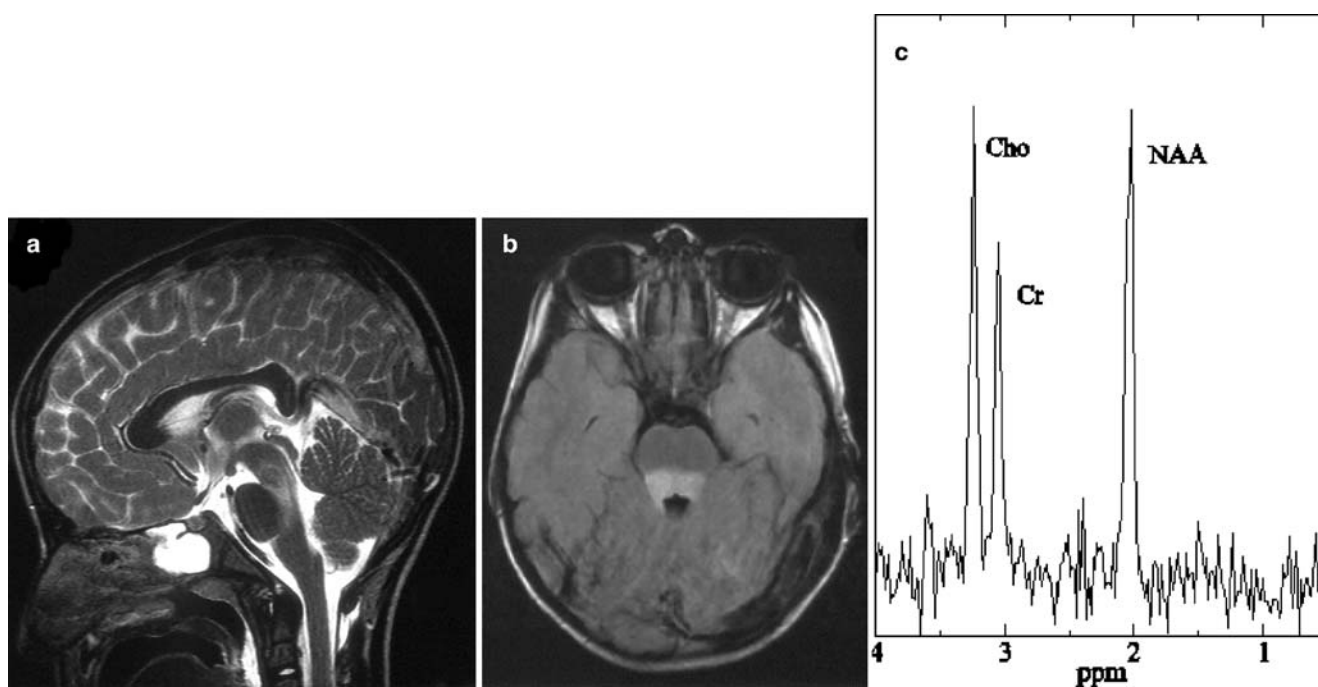
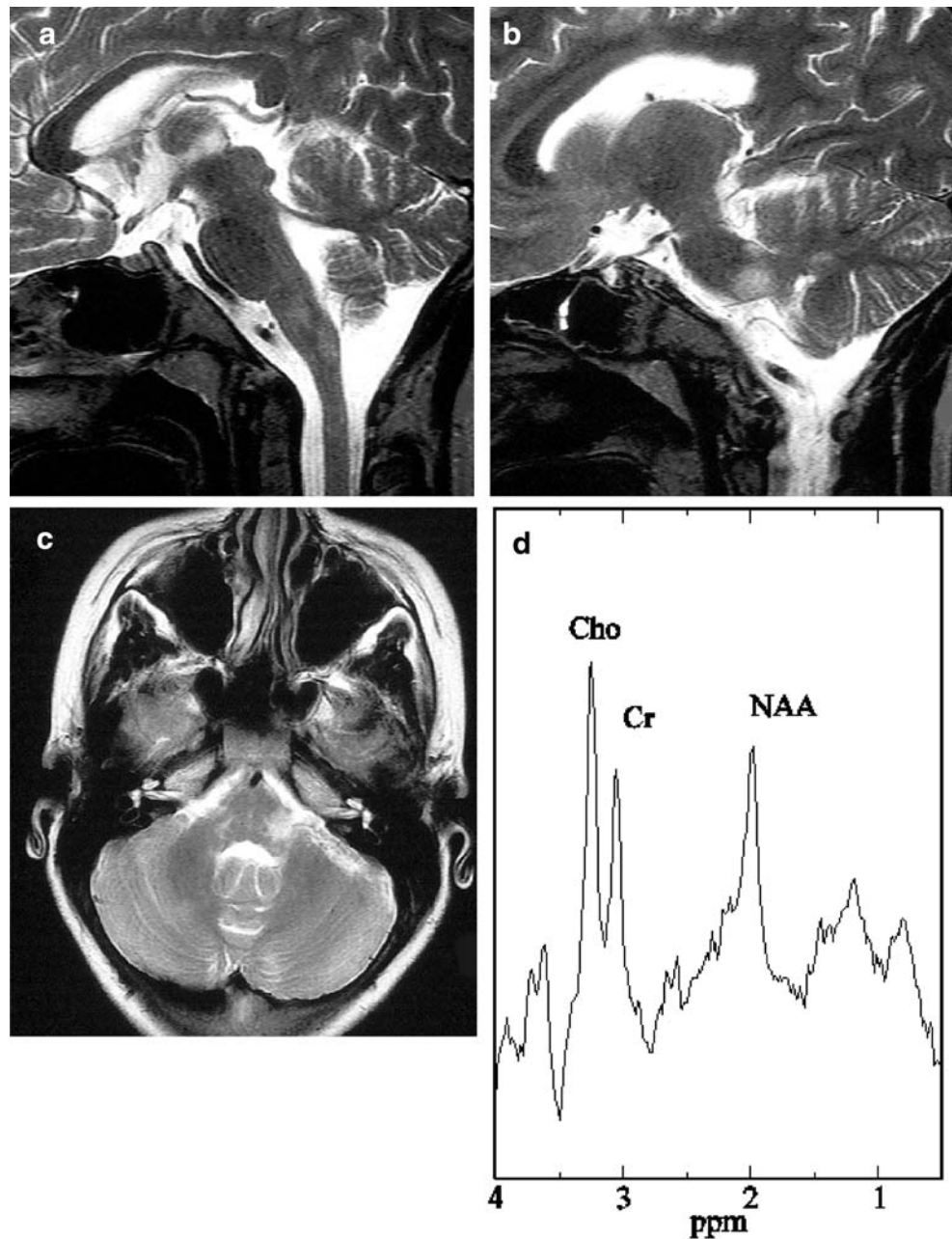


Fig. 3 A 5-year-old boy presented with sudden onset of sixth nerve palsy and disequilibrium. **a** Sagittal T2-weighted image shows a diffuse area of hyperintensity in the posterior half of the pons with cranial extension to the tegmentum of the mesencephalon. The

hyperintense T2-weighted MR imaging signal has fully regressed in 1 week (not shown). **b** FLAIR image obtained through the pons shows a well-defined area of hyperintensity in the tegmentum. **c** Normal spectrum of brain stem lesion

Fig. 4 An 11-year-old right-handed girl with acute right-sided hemiparesis and disequilibrium. Oligoclonal bands were positive in this patient confirming the diagnosis of MS. **a, b** Sagittal T2 images show abnormal signals on the left side of the brainstem and middle cerebellar peduncle. **c** Axial T2-weighted MR image shows the hyperintense area on the left side of the brainstem with extension to the middle cerebellar peduncle. **d** Spectrum of brain stem mass lesion. Values of NAA (2.0 ppm), Cr (3.0 ppm), and Cho (3.2 ppm) reflect signal peak integrals (arbitrary units). Metabolite levels relative to the contralateral normal cerebellum: NAA 41%; Cho 118%. No lactate peak. Levels of NAA are decreased while Cho are mildly elevated, which is compatible with demyelinating disease



was low. The high Cho peak was suggestive of high-grade astrocytoma. Primitive neuroectodermal tumor (PNET) was included in the differential diagnosis. It has been reported previously [12] that a significant decrease of Cr signal intensity was present in PNET compared to low- and high-grade astrocytomas. Therefore, the NAA/Cr ratio of PNET tumors [12] was also significantly higher compared to gliomas. Based on the relative high Cr level, we favored the diagnosis of a high-grade astrocytoma. This was confirmed by open biopsy.

The cases of patient 3 and patient 4 suggest that MRS may have a role in the differential diagnosis of acute disseminated encephalomyelitis (ADEM). During the acute

phase of demyelination in multiple sclerosis (MS) and of various leukodystrophies, choline levels are usually elevated [3]. The increased “choline” signal is believed to result from increased levels of the myelin breakdown products—glycerophosphocholine and phosphocholine. In patient 3 and in other previously reported cases of ADEM [16] studied with MRS, the choline signal was normal, and the region of interest was hyperintense on T2-weighted sequences. Over time, the hyperintense signal gradually resolved (patient 3). Abnormal hyperintense T2-weighted signal with normal levels of choline may indicate that the underlying pathologic process is related more to the local edema than to demyelination. In this setting, a normal

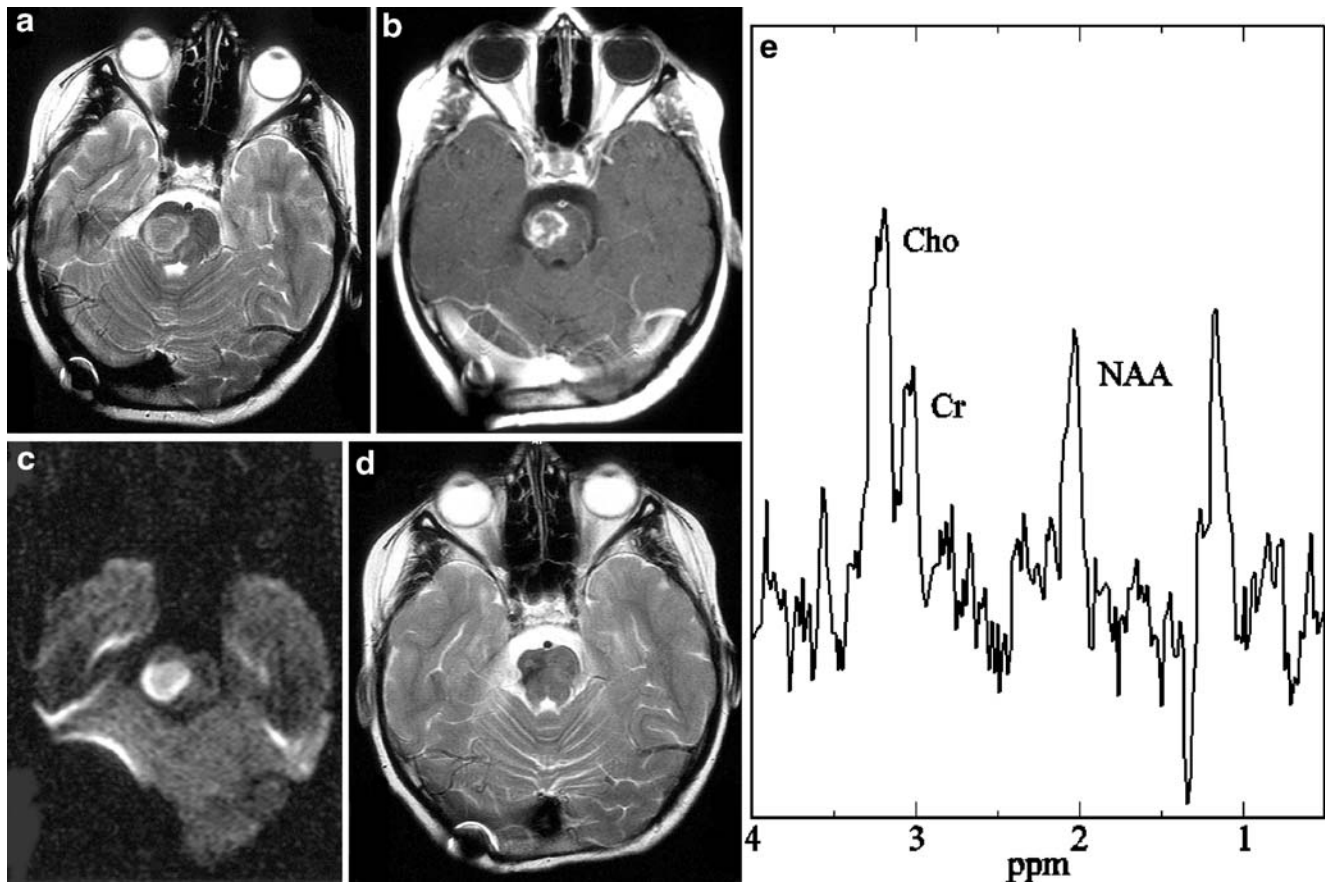


Fig. 5 A 15-year-old girl was admitted with a history of left-sided hemiparesis and disequilibrium. **a, b** Axial T2 and T1 after contrast images show a round hyperintense signal in the right upper pons with a ring-like enhancement after contrast. **c** Axial diffusion-weighted image show the hyperintense pontine lesion. **d** After 6 months, axial T2 image shows some residual changes in the pons,

which are mildly hypointense. **e** Spectrum of brain stem mass lesion. Values of NAA (2.0 ppm), Cr (3.0 ppm), and Cho (3.2 ppm) reflect signal peak integrals (arbitrary units). Metabolite levels relative to the normal cerebellum: NAA 32%; Cho 86%. A lipid-dominant peak is observed in the spectrum, as well as moderate amounts of lactate

choline level might have prognostic implications for recovery, a hypothesis that is potentially of great value but will require testing in a larger cohort of patients [3]. Another important disorder in the differential diagnosis of ADEM is mitochondrial encephalomyopathy. It has been reported that mitochondrial diseases [3] have elevated cerebral and CSF lactate levels on MRS. In the case of patient 3, the absence of lactate in the region of interest and CSF was helpful in downgrading the diagnostic likelihood of mitochondrial encephalopathy. Elevated lactate levels have been reported in mitochondrial encephalopathies such as mitochondrial encephalopathy, lactic acidosis, and stroke (MELAS); myoclonic epilepsy and ragged fibers (MERFF); Kearns-Sayre syndrome; and Leigh disease. However, the sensitivity and specificity of the spectroscopic detection of lactate as a diagnostic test for these and other mitochondrial diseases remain to be determined. Small elevations of lactate have also been reported in fulminant demyelinating lesions [3] but were not observed in our cases (patient 3 and patient 4).

NAA levels are decreased in lesions known to involve neuronal and axonal loss (e.g., infarcts, brain tumors, seizure foci, MS plaques). Therefore, it has been suggested that the NAA signal may be used as a marker of permanent neuronal or axonal loss. However, it is now becoming apparent that, as for other amino acids, NAA levels depend not only on neuronal density but also on fluxes of synthetic and degradation pathways [3]. A case report of a 2-year-old child with mental retardation and normal brain MR imaging findings describes a complete absence of cerebral NAA [17], presumably resulting from a defect in the synthetic pathway of NAA. Therefore, decreased levels of NAA should not automatically be interpreted as resulting from neuronal/axonal loss or viability. Reversible NAA decreases have been demonstrated in patients with single transient acute demyelinating MS lesions, in patients with mitochondrial encephalopathy and in one patient with ADEM [3]. In patients with a single large demyelinating lesion, De Stefano et al. [6] found a 34% to 45% NAA

deficit during the acute phase of the disease, followed by almost complete NAA recovery (70% to 80% of the normal contralateral NAA levels).

It is often difficult to make the correct diagnosis of ring-like enhanced lesions on gadolinium-enhanced MR brain images, as in the case of patient 5. The appearance of a new lesion 8 years after radiation treatment for primary brain tumor may represent recurrence of the tumor, infection, radiation-induced demyelination [2, 15], radiation necrosis of the brain, ischemic stroke secondary to radiation-induced vasculopathy, secondary tumor, or occult vascular malformation. We believe that tumor recurrence was unlikely in our patient. The pontine lesion was remote from the tumor's primary site, and PET did not show increased uptake and spectroscopy did not show any choline peak. Pontine infarction was suggested by the initial MRI. However, the follow-up MR images argued against it in that a typical ischemic infarct should develop into a lacunar defect. Spectroscopy showed a high lipid-dominant peak, as evidence of necrosis at the level of the pons. On the other hand, the presence of hypointense areas on the T2-weighted images, compatible with small areas of hemorrhage, favors the diagnosis of radiation-induced necrosis.

Previous MRS studies [7, 9] of radiation necrosis have shown the presence of a high lipid-dominant peak, low NAA peak, and a lower Cho peak compared with metastasis or glioblastoma. The lipid-dominant peak may reflect the presence of the necrotic part of the radiation necrosis. Fulham et al. [7] reported that a high lactate-dominant peak was observed in subacute radiation necrosis.

In the subacute phase of cerebral infarction, a ring-like enhanced lesion with mild swelling is found in MR images, and it is difficult to differentiate them from tumors. Typical of cerebral infarction is the lactate peak. As in the case of radiation necrosis, lipid-dominant peaks have been observed from the central nonenhanced region in the cerebral infarction cases [9].

MRS helped in the case of patient 5 to rule out recurrence, that is, proliferative process. Unfortunately, the final diagnosis remains unclear in this case.

Conclusion

MRS plays a major role in the evaluation of brainstem lesions. We believe that MRS is important in the differential diagnosis between proliferative and nonproliferative lesions in patients without neurofibromatosis.

Unfortunately, in cases of NF 1, MRS can have a rather misdiagnosis role. In situations such as NF 1, Cho peak should not necessarily be considered as a sign of a high malignant lesion. With the knowledge of child's age, MRS controls should be performed, thereby minimizing aggres-

sive treatment and its side effects in patients destined to have better outcomes than patients with diffuse pontine gliomas.

References

- Barkovich AJ (2005) Pediatric neuroimaging, 4th edn. Lippincott-Raven, Philadelphia, pp 321–347
- Biousse V, Newman NJ, Hunter SB et al (2003) Diffusion weighted imaging in radiation necrosis. *J Neurol Neurosurg Psychiatry* 74:382–384
- Bizzi A, Ulug AM, Crawford TO et al (2001) Quantitative proton MR spectroscopic imaging in acute disseminated encephalomyelitis. *AJNR Am J Neuroradiol* 22:1125–1130
- Castillo M, Green C, Kwock L et al (1995) Proton MR spectroscopy in patients with neurofibromatosis type 1: evaluation of hamartomas and clinical correlation. *AJNR* 16:141–147
- Curless RG, Bowen BC, Pattany PM et al (2002) Magnetic resonance spectroscopy in childhood brainstem tumors. *Pediatr Neurol* 26(5):374–378
- De Stefano N, Matthews PM, Arnold DL (1995) Reversible decreases in N-acetylaspartate after acute brain injury. *Magn Reson Med* 34:721–727
- Fulham MJ, Bizzi A, Dietz MJ et al (1992) Mapping the brain tumor metabolites with proton MR spectroscopic imaging: clinical relevance. *Radiology* 185:675–686
- Jones AP, Gunawardena WJ, Coutinho CM (2001) 1H MR spectroscopy evidence for the varied nature of asymptomatic focal brain lesions in neurofibromatosis type 1. *Neuroradiology* 43(1):62–67
- Kimura T, Sako K, Tanaka K et al (2001) In vivo single-voxel proton MR spectroscopy in brain lesions with ring-like enhancement. *NMR Biomed* 14:339–349
- Kruger MD, Blüml S, McComb JG (2003) Magnetic resonance spectroscopy of atypical diffuse pontine masses. *Neurosurg Focus* 15(1):E5
- Laprie A, Pirzkall A, Haas-Kogan DA et al (2005) Longitudinal multivoxel MR spectroscopy study of pediatric diffuse brainstem gliomas treated with radiotherapy. *Int J Oncol Biol Phys* 62(1): 20–31
- Möller-Hartmann W, Herminghaus S, Krings T et al (2002) Clinical application of proton magnetic resonance spectroscopy in the diagnosis of intracranial mass lesions. *Neuroradiology* 44:371–381
- Nafe R, Herminghaus S, Raab P et al (2003) Preoperative proton-MR spectroscopy of gliomas-correlation with quantitative nuclear morphology in surgical specimen. *J Neurooncol* 63:233–245
- Naressi A, Couturier C, Devos JM et al (2001) Java-based graphical user interface for the MRUI quantitation package. *MAGMA* 12:141–152
- Park SH, Chang KH, Song IC et al (2000) Diffusion-weighted MRI in cystic or necrotic intracranial lesions. *Neuroradiology* 42:716–721
- Tan HM, Chan LL, Chuah KL et al (2004) Monophasic, solitary tumefactive demyelinating lesion: neuroimaging features and neuropathological diagnosis. *Br J Radiol* 77(914):153–156
- Thiel T, Capone A, Schneider JF et al (2000) N-acetylaspartate: a marker for viable neurons? [abstract]. In: Book of International Society for Magnetic Resonance in Medicine's (ISMRM's) 8th Scientific Meeting and Exhibition. Denver, CO, ISMRN, p 1909
- van den Boogaart A, van Ormondt D, Pijnappel WWF et al (eds) (1994) Mathematics in signal processing III. Clarendon Press, Oxford, pp 175–195
- van den Boogaart A, Van Hecke A, Van Huffel P et al (1996) MRUI: a graphical user interface for accurate routine MRS data analysis. p 318

20. van den Boogaart A (1997) MRUI MANUAL V. 96.3. A user's guide to the magnetic resonance user interface software package. Delft Technical University Press, Delft
21. Vanhamme L, van den Boogaart A, Van Huffel S (1997) Improved method for accurate and efficient quantification of MRS data with use of prior knowledge. *J Magn Reson* 129:35–43
22. Wang PY, Kaufmann WE, Koth CW et al (2000) Thalamic involvement in neurofibromatosis type 1: evaluation with proton magnetic resonance spectroscopic imaging. *Ann Neurol* 47(4):477–484
23. Warren KE, Frank JA, Black JL et al (2000) Proton magnetic resonance spectroscopy imaging in children with recurrent primary brain tumors. *J Clin Oncol* 18:1020–1026
24. Zoula S, Herigaut G, Ziegler A et al (2003) Correlation between the occurrence of 1H-MRS lipid signal, necrosis and lipid droplets during C6 rat glioma development. *NMR Biomed* 16(4):199–212